

<https://doi.org/10.1364/JOSAA.23.002880>

Determination of optical constants of Sc films in the 20-1,000-eV range

Mónica Fernández-Perea, Juan I. Larruquert, José A. Aznárez, José A. Méndez

Instituto de Física Aplicada-Consejo Superior de Investigaciones Científicas, C/ Serrano

144, 28006 Madrid, Spain, phone: 34 91 561 8806; fax: 34 91 411 7651, email:

larruquert@ifa.cetef.csic.es

Luca Poletto

Dep. of Information Engineering, Laboratory for UV and X-Ray Optical Research -

Istituto Nazionale per la Fisica della Materia, Padua, Italy

A. Marco Malvezzi

Dipartimento di Elettronica, Università di Pavia and INFN, Via Ferrata, 1, I27100

Pavia, Italy

Angelo Giglia, Stefano Nannarone

TASC-INFN-CNR, s. s. 14, km 163.5 in Area Science Park, I-34012

Trieste, Italy

The transmittance of thin films of Sc deposited by evaporation in ultra high vacuum conditions have been investigated in the 20-1,000 eV spectral range. Transmittance measurements were performed in situ on Sc layers that were deposited over grids coated with a C support film. Transmittance measurements were used to obtain the extinction coefficient of Sc films at each individual photon energy investigated. These data, along with the data available in the literature for the rest of the spectrum, were used to obtain

the refractive index of Sc by means of the Kramers-Krönig analysis. Sum-rule tests indicate an acceptable consistency of the data.

OCIS Codes: 260.7200 Ultraviolet, extreme; 230.4170 Multilayers; 120.4530 Optical constants; 350.2450 Filters, absorption; 310.6860 Thin films: optical properties

1. INTRODUCTION

Sc is a material that has demonstrated a good performance as a component of multilayers for the extreme ultraviolet¹ and soft x-rays² at specific bands with photon energies smaller than the Sc M_{2,3} edge (28.3 eV) and L_{2,3} edge (403.6, 398.7 eV). Surprisingly, these multilayers have been developed without a precise knowledge of the optical constants of Sc at the design wavelength. Hence a better knowledge of the optical constants of Sc is expected to provide multilayers with a larger reflectance. The transmittance characteristics of Sc may also result in a new potential application of Sc films as transmission filters, with a transmittance band at ~20-30 eV in which there is a shortage of materials with adequate transmission bands.

Scarce literature has been available on the optical properties of Sc in the EUV until recently. Optical measurements on any kind of Sc samples had been restricted to energies smaller than 5.5 eV: Weaver and Olson³ measured absorption on single Sc crystals in the 0.2-5 eV range, and Sigrist et al.⁴ measured near normal reflectivity of Sc films in the 0.22-5.5 eV range. Electron energy-loss (EEL) measurements were performed on Sc samples by Brousseau-Lahaye et al.⁵, which were used to calculate the complex dielectric constant of Sc films in the ~6.2-55.1 eV range through the Kramers-Krönig (KK) analysis. In the latter work, sample preparation and handling is not clear, so that contamination, if present, may result in errors in the determination of the optical constants. Theoretical calculations of the optical constants of Sc in the EUV have been performed by Uspenskii et al.⁶.

The importance of Sc as a component of multilayers has recently attracted interest on the characterization of Sc in the EUV and soft x-rays. Uspenskii et al.⁷ and Aquila et al.⁸

have recently characterized the optical properties of Sc in the 18-70 and 50-1300 eV, respectively, with the use of synchrotron radiation. In ref. 7, silicon photodiodes were coated with Sc of various thicknesses, and they were protected with a 5-nm thick Si film; the radiation transmitted through the Sc plus Si was measured ex situ and it gave a measurement of the transmittance of these layers, from which the extinction coefficient was obtained. The refractive index was calculated through the KK analysis that also took into account reflectance measurements. In ref. 8, the transmittance of free-standing Si/Sc/Si trilayers was measured ex situ; the trilayers were deposited onto photoresist-coated wafers, and the photoresist was later dissolved by soaking in acetone. The dispersion of Sc films was also obtained with the KK analysis. The two above studies encompass protective coatings, and the latter even some layer dissolution and contact with solvents, which might be a source of contamination and complicate the interpretation of the measurements. Hence, in situ measurements on Sc films are desirable both to provide with new data and to confirm that the above data are not affected by the presence of protective coatings and/or by the exposure to the atmosphere or to solvents. Larruquert et al.⁹ performed reflectance and transmittance measurements over in situ-deposited Sc films in ultra high vacuum conditions at several spectral lines of the 7.11-23.13-eV range, which enabled the direct determination of the optical constants at each photon energy; they also measured ex situ the transmittance of C/Sc/C sandwiches supported on grids at several spectral lines and bands between 42 and 185 eV.

The current paper reports on the in situ characterization of the optical constants of Sc films in the spectral range from 20 to 1,000 eV from transmittance measurements in the above range. The characterization is completed with the KK analysis both to calculate

the dispersion of Sc and to check the consistency of the data. The current data, along with the data published in Ref. 9 extends the available data that have been obtained in situ to the combined range 7.11-1,000 eV. The experimental techniques used are described in Section 2. Section 3 reports the experimental data and the KK analysis.

2. Experimental techniques

2.1 Sample preparation

Deposition of thin films for transmittance measurements requires special substrates because of the lack of materials with a high transmittance in the spectrum of interest. The special substrates used in this research consist of a microgrid of relatively high transmittance on which a thin film of a material with suitable transmittance is deposited. This thin film supports the scandium layers for transmittance measurements. The microgrid provides mechanical support for the deposited layers. We used an electroformed hexagonal nickel grid of 750 mesh (hole: 25 μm ; bar: 8 μm , thickness: 0.875 μm) from Stork-Veco with a transmittance of about 50%. Grid pieces were epoxy glued on molybdenum sheet frames. The usable area was 10x10 mm².

We prepared thin film substrates consisting of carbon films of ~10-nm thickness that were deposited by evaporation using a Balzers electron gun at a pressure of $\sim 10^{-6}$ mbar. C films were used because very thin films of this material are known to result in a continuous, hole-free layer. Carbon films were deposited onto freshly cleaved mica. The carbon film was floated off on water and the film was lifted carefully with the microgrid-on-frame, which had been previously dipped in the water. After drying at room temperature the carbon film adheres to the microgrid. These carbon thin films are very fragile and must be handled with care.

Three Sc layers were deposited successively onto a single substrate. The sample was transferred back and forth between the deposition chamber and the measurement chamber, always under UHV, for the deposition of a new layer and its characterization. We used a TriCon evaporation source¹⁰, in which the 99.999% purity scandium lumps (Stanford Materials) were placed in a small tungsten crucible that was heated by electrons coming from a surrounding filament. Sc films were deposited onto room-temperature substrates. The distance from the source to the carbon substrate was 10 cm. We placed the substrate close to a witness piece of glass partially covered with a blade for ex situ thickness measurement. The deposition rate was controlled in situ with a quartz monitor, and, ex situ through Tolansky interferometry, i.e., through multiple-beam interference fringes in a wedge between two highly reflective surfaces¹¹. Deposition rate was maintained at 2-3 nm/minute for all the evaporations.

2.2 Experimental setup for transmittance measurements

The transmittance measurements were performed at the BEAR beamline at Elettra Synchrotron (Trieste, Italy), which operates in the energy range from 3 to 1,600 eV, and consists of a monochromator and of an experimental station. The monochromator has three different channels with gratings illuminated in parallel light, two of them with optics at grazing incidence and one at normal incidence.

The whole 20-1,000-eV spectral range has been covered with two channels: the NIM (Normal-Incidence Monochromator) channel, working at fixed deviation angle to cover the UV region (20-50 eV), and the G1200 channel, working at grazing incidence and at selectable deviation angle for the 40-1,600 eV energy range¹². Being transmittance

measurements at normal incidence independent of the degree of polarization of light, we measured full beam, corresponding to a degree of linear polarization of about 0.5. With the used slit configuration, the monochromator spectral broadening is of about 0.1 eV in the range 20-200 eV and of about 0.5 eV in the range 200-1000 eV (0.2-0.3 eV at the Sc L edge). The suppression of higher orders has been achieved using Al and Si filters below 100 eV, and choosing the appropriate deviation angle at higher energies. The spot size on the sample was $0.4 \times 0.2 \text{ mm}^2$.

The measurements were performed at the BEAR spectroscopy chamber¹³, connected in vacuum ($P=1.3 \times 10^{-10}$ mbar) to the preparation chamber, where in-situ samples were prepared. The transmission and their relative direct signals have been measured using as a detector an IRD AXUV-100 silicon photodiode¹⁴. The correction of the background signal has been done by measuring the dark signal of the photodiode, and possible fluctuations of the photon beam have been recorded with a 100 V biased W-mesh. The normalization of the measurements has been done by taking into account the mesh or the ring current. Being the differences between the two kinds of normalizations 2% at maximum, apart from the region of overlapping of the two monochromator channels (40-50 eV) and at higher energies (> 800 eV), where the mesh signal was too noisy, we used data normalized with the ring current through:

$$T = \frac{(I_T - I_B) / R_T}{(I_D - I_B) / R_D} \quad (1)$$

where I_T and I_D represent the diode currents given by the transmitted and direct beam, respectively, I_B represents the background diode current, and R_T and R_D represent the ring current during the measurement of the transmitted and direct beam, respectively.

3. Results and discussion

3.1 Transmittance data and the extinction coefficient

The experiment was performed by making several sets of measurements on a grid-supported C film over which three film depositions were made. First of all, the uniformity of the substrate was verified inside the central region of the sample (4×4 mm²). The transmittance of the substrate is shown in Fig. 1, where the strong absorption of C K edge around 285 eV and the tail coming from the C L edge at 15-20 eV are well evident.

We performed three consecutive depositions on the substrate; the layer thicknesses were 63, 155, and 205 nm. A comment on the thickness determination is included in the next subsection. The transmittance curves of the three films are shown in Fig. 2, in which the contribution of the substrate has been subtracted. For each of the three films we verified the uniformity inside the central region with two different photon energies: 20 and 200 eV. The variation of transmittance signal has been verified less than 3% at 20 eV and less than 0.4% at 200 eV. In any case, the sample has been positioned for the three sets of measurements in the same position within an uncertainty of 0.5 mm. This has been achieved by placing the detector at the same position, after having verified that the absolute uncertainty due to the detector was about 1%. Then, we can estimate that the overall uncertainty in the transmittance measurements is of the order of 3-4%

Transmittance is related to the extinction coefficient k (the imaginary part of the complex refractive index $N=n+ik$), of the material through:

$$\frac{T_{fs}}{T_s} \approx \exp\left(-\frac{4\pi kx}{\lambda}\right) \quad (2)$$

where T_s and T_{fs} represent the transmittance of the uncoated substrate and of the substrate coated with a Sc film, respectively. x stands for the Sc film thickness. So, a good check of the quality of the measurements is given by the plot of the logarithm of transmittance, which must be linear with respect to the film thickness; some examples are given in Fig. 3. In the whole spectral range we verified a good linearity, except in the valleys relative to the L and M absorption edges, where transmittance data for the second and third depositions were comparable with higher order contribution. For this reason, in these two regions we used the data coming only from the first film deposition, where the higher order contribution has been verified of the same order of the measurement error.

Eq. (2) neglects the reflectance of the sample. The theoretical normal incidence reflectance of the scandium films was calculated after the determination of the optical constants n and k ; this reflectance is absolutely negligible for energies higher than 40 eV and it is less than 4% in the 20-40 eV region. Taking and not taking into account the reflectance in the extinction coefficient calculation from transmittance measurements results in a maximum difference in the extinction coefficient of less than 0.5% at the 20-40 eV, which is lower than the overall uncertainty.

The transmittance as a function of thickness was used to obtain the extinction coefficient of Sc. A log-log plot of this coefficient versus photon energy is displayed in Fig. 4. The average of the three depositions was used, except at the M and L edges, where only the first deposition was considered. The Sc $M_{2,3}$ and $L_{2,3}$ edges are strongly evident. In the spectral range 80-200 eV we can observe clear oscillations that we ascribed to a NEXAFS signal above the M edges of scandium, which will be more

carefully described in a forthcoming paper. The little transmittance peak at 285 eV (Fig. 2), relative to C 1s, is probably due to C contamination of the scandium films or to a residual signal from the carbon of the substrate, not uniformly distributed over the nickel mesh. We evaluated the ratio between residual carbon and scandium being around 4%, by comparing the experimental data with the calculated mass absorption coefficient of C and Sc. This extra carbon signal was considered to affect in a negligible manner the consistency of the transmittance measurements by observing the transmittance both below and above the C K edge, and hence we interpolated the optical constants by smoothly connecting the surrounding areas; Fig. 4 displays the data with that interpolation. Instead, there are no significant evidences of oxygen contamination at O K edge at about 540 eV.

For comparison purposes, the data available in the literature^{7,8,9} along with data calculated with the semi-empirical approach of Henke et al.¹⁵ has been also plotted in Fig. 4. The Henke data for the extinction coefficient of Sc was calculated using the web page of the Center for X-Ray Optics (CXRO) at Lawrence Berkeley National Laboratory¹⁶. The Henke approach depends on the density of the material. Being the extinction coefficient, as calculated from atomic scattering factors, proportional to the density of the material, we experimentally measured the density of Sc films in the following way. We measured the density of Sc films by depositing Sc films on Al foils that were weighed before and after Sc deposition. Sc film thickness was measured by Tolanski interferometry on witness samples. We obtained a density of $2.84 \pm 0.06 \text{ g/cm}^3$, versus 2.985 g/cm^3 for bulk Sc. The former was used in the Henke approach.

The current data overlap those of Uspenskii et al.⁷ and Aquila et al.⁸. There is a good

match with the two sets of data. Uspenskii's data seem to diverge at the high energy limit (75 eV). A scale difference is observed with Aquila's data at the Sc L_{2,3} edge, which is highlighted in Fig 5. This and other differences pointed out between Aquila's and the current data might be in part due to the fact that the latter data were obtained on Sc samples deposited by DC magnetron sputtering, whereas the current samples were prepared by evaporation. There is a difference with Uspenskii's data around the wide M edge, which suggests an energy shift of roughly 2 eV. The connection with Larruquert's data⁹ is good. Henke data does not reproduce accurately the experimental data at energies close to the M and L edges, as expected. There are oscillations also above the L_{2,3} edge, which we ascribed to a NEXAFS signal that also will be described in a forthcoming paper.

3.2 Refractive index calculation with the dispersion relations

The dispersion of Sc was calculated with the KK dispersion relations:

$$n(E) - 1 = \frac{2}{\pi} P \int_0^{\infty} \frac{E' k(E')}{E'^2 - E^2} dE' \quad (3)$$

where P stands for the Cauchy principal part. One difficulty of the above equation is the necessity of k data over the whole spectrum. With most materials, the data come from different sources, different sample preparation, etc., which results in inaccuracies when obtaining n with Eq. (3). The available data for Sc encompasses the current data in the 20-1,000 eV, along with the in situ data of Larruquert et al.⁹ in the 7.1-23.1 eV, which were used below 20 eV; in both cases the data were obtained from either reflectance or transmittance measurements on thin films prepared in situ. Between 1,000 and 30,000 eV we used Henke data from CXRO's web. The extrapolation to infinity was performed by keeping constant the slope of the log-log plot of $k(E)$ in the Henke data.

At smaller energies, we used the optical constants of thin films obtained by Sigrist et al.⁴ from in situ reflectance measurements in the 0.27-5.5 eV; even though measurements were performed from 0.22 eV, data on ϵ_1 was plotted above 0.27 eV. They calculated the optical constants of Sc from these reflectance data using a KK analysis with the data available at that time, and the authors used reflectance data at larger energies coming from samples that had been exposed to the air; hence Sigrist's data may have a limited accuracy. A linear extrapolation was here used to fill the gap between 5.5 and 7.1 eV.

Weaver and Olson³ measured the absorption of a single hcp Sc crystal in the 0.2-5 eV. The optical constants of Weaver and Olson³ were published in the compilation of Weaver et al.¹⁷, where data from 0.1 eV, and not from 0.2 eV, are available. The data of Ref. 17 were used in the 0.1-0.27 eV range. Since Sc crystals are uniaxial, two sets of optical constants were published by Weaver and Olson, which corresponded to the electric field of the incident radiation being parallel or perpendicular to the optics axis of the crystal. Several difficulties arise in the use of Weaver and Olson's data in the current case: there are two sets of data instead of one, and the sample presentation and the type of measurements are different.

Evaporated thin films of Sc are polycrystalline, and they are formed by a large number of small crystallites¹⁸. Hence, it can be suggested that the effective optical constant data of a Sc film should be a certain combination of the two sets of data available for single crystals. Such an average would require specifying the crystalline orientation of the Sc films, in order to discriminate whether the orientation is completely random or there

exists some preferred orientation. In order to assess this point we observed Sc films by transmission electron microscopy (TEM) and obtained electron diffraction patterns of large areas of the films. The absence of (002) reflections in the patterns, which only appeared after a pronounced sample tilting of about 45° , suggests that crystallites have their c axis roughly between the perpendicular to the surface of the film and 45° from it.

The next step is to assess the method to average out the two sets of optical constants for the current distribution of crystal orientations. In the close literature involving the KK analysis of thin films in which some data correspond to uniaxial single crystals, an undetermined selection or average of optical constants has been used^{8,19}. Several theories, such as the Maxwell-Garnett theory and the Effective Medium Approximation (EMA), have been proposed to model the optical constants of non-cubic polycrystalline materials starting with the single crystal dielectric tensor. To the authors' knowledge, no theory has been proposed to model one optical constant, such as the extinction coefficient in polycrystalline uniaxial crystals, in order to perform specifically the KK analysis.

A new method of modeling the infrared spectra of non-cubic polycrystalline materials has been proposed by Mayerhöfer²⁰ consisting in the average of the complex refractive index over all crystallite orientations. The theory is developed assuming that the ordered regions (crystallites) are smaller than the resolution limit of one tenth of the radiation wavelength. Ref. 20 applies the method to fresnoite, with excellent correspondence between simulated and measured spectra compared to an inferior match obtained with EMA; the latter method involves an average of the dielectric constant instead of the refractive index. Mayerhöfer's method was selected here and the average was

performed using Eq. (12) of Ref. 20. The average in Ref. 20 was performed in the whole hemisphere assuming random crystallite orientation; in our case, the polar angle was allowed to take values only between 45° and 90° from the film surface, according to the aforementioned crystallite distribution. The crystallite size of our Sc films satisfies well Mayerhöfer's resolution limit, which is $4.6 \mu\text{m}$ for the 0.1-0.27 eV range.

The extrapolation to zero energy was performed using a Drude model. Drude parameters were optimized to better connect with the short energy limit of the data collection (Weaver and Olson's data). The following parameters were obtained: $\lambda_p=455 \text{ nm}$, $\tau=1.56 \times 10^{-14} \text{ s}$.

Fig. 6 displays the data of the extinction coefficient that were gathered for the KK analysis, except for the extrapolation regions. Figs. 7 to 9 display $\delta=1-n$ calculated with Eq. (3).

Similar to what was obtained with k data, a scale difference with Aquila's data is observed for δ at the Sc $L_{2,3}$ edge. Other than this, Aquila's data are somewhat smaller than the current data for energies smaller than the Sc L edge. The current data and Aquila's data display similar weak oscillations peaked at the same energies ranging between 430 and 550 eV both in k and δ . There is a reasonable coincidence with Uspenskii's data in δ , with an energy shift at the M edge that is similar to the one already presented for k data. Henke data peak is positioned at the same energy that for the current data.

The optical constant data at the energy of smallest absorption both below the L and M edges are given in Table 1²¹.

Sum-rule tests provide a valuable guidance to evaluate the accuracy of the dispersion analysis. The f -sum rule relates the number density of electrons to the dissipative or imaginary part of the refractive index²². This sum-rule can be written as:

$$\int_0^{\infty} E' k(E') dE' = \frac{\pi N_{el} e^2 h^2}{4 \epsilon_0 m} \quad (4)$$

where N_{el} is the electron density, e is the electron charge, ϵ_0 is the permittivity of vacuum, m is the electron mass, and h is Planck's constant. It is useful to define the effective number of electrons contributing to the optical properties up to a given energy as:

$$n_{eff}(E) = \frac{4\epsilon_0 m}{\pi N_{at} e^2 h^2} \int_0^E E' k(E') dE' \quad (5)$$

where N_{at} is the atom density. In the limit of high energy n_{eff} must converge to the number of electrons of a Sc atom. The differences in Eqs. (4) and (5) with the equations present in Ref. 22 arise in that we used here the international system of units instead of CGS.

The high energy limit of the effective number of electrons must reach 21, the atomic number of Sc. In order to calculate this value, we initially used the thickness data that had been calculated involving Tolanski interferometry; these measurements were performed ex situ, so that some slight variation of the real thickness when the Sc sample was exposed to atmosphere cannot be discarded. Tolanski measurements resulted in a total thickness estimation of 216 nm; this value is the extrapolation of the thicknesses measured at different spots of the witness sample towards the position of the spot in the

sample where transmittance measurements had been performed. This extrapolation results in some thickness uncertainty too. The thickness of the first two depositions could not be measured independently because the witness accumulated the three depositions without information of the individual depositions. If we take logarithms on Eq. (2) and divide the results for two thicknesses, the right term equals a thickness ratio, whereas the left term can be calculated with the current transmittance data. We operated in this way for the large energies of the spectrum and obtained thickness ratios, which along with the total thickness datum, provided us with the thicknesses of the three layers whose transmittance was measured. We obtained the following thicknesses: 66, 163, and 216 nm. With these thickness data we calculated k and obtained an effective number of electrons of 19.4, which is 7.5% lower than expected. This uncertainty could be attributed partly to the uncertainty in thickness, according to the above discussion.

In order to improve the consistency of the data, we recalculated the layer thicknesses in the following way. We fitted the large energy transmittance data of the three Sc thicknesses with Henke data using the Sc density that was reported in subsection 2.1 (2.84 g/cm^3). This procedure gave us the three following layer thicknesses: 63, 155, and 205 nm. We recalculated k and obtained an effective number of electrons of 20.3, which is 3.3% lower than expected. The latter thicknesses are within the estimated thickness uncertainty of those calculated starting with Tolanski interferometry (within 5%), and they result in an effective number of electrons considerably closer to the correct value. Therefore, we used the thickness data calculated in the fitting with the Henke approach throughout this paper, and the k data so obtained are plotted in Figs. 4 to 6, which were used to calculate the δ data reported in Figs. 7 to 9.

Fig. 10 displays the effective number of electrons contributing to the imaginary part of the refractive index of Sc. The integration was performed in the whole spectrum, and Fig. 10 only plots the part of the spectrum contributing to the sum-rule test in a non-negligible amount. The main contribution to n_{eff} comes from the 1-30,000 eV range, which has been mostly covered with in situ data and with the Henke data for large energies; the latter data are expected to be accurate since they are well within a valid energy range. The data below 7 eV are probably less reliable, as explained above.

Another useful test to evaluate the accuracy of the KK analysis is obtained with the inertial sum-rule:

$$\int_0^{\infty} [n(E) - 1] dE = 0 \quad (6)$$

In practice it must be defined some way of evaluating whether the calculated integral of Eq. (6) is or is not close enough to zero. According to Shiles et al.²², the following evaluation parameter was used:

$$\zeta = \frac{\int_0^{\infty} [n(E) - 1] dE}{\int_0^{\infty} |n(E) - 1| dE} \quad (7)$$

Shiles et al.²² used the above parameter in the analysis of Al and obtained $\zeta = -0.002$.

They mention some other work on Al in which ζ takes a value as high as 0.17, which demonstrates a large inconsistency of the analysis. They suggest that a good value of ζ stands within ± 0.005 . The sum-rule test in the current case resulted in $\zeta = -0.008$, which even though out of the top value proposed by Shiles et al., it is considered acceptable here, taking into account the large number of data sources (some of them involving ex situ measurements) that had to be used in the current dispersion analysis. We suggest

that new in situ characterizations below 7 eV may still somewhat improve the consistency of the KK analysis.

In conclusion, by a careful selection of data in the literature and critical evaluation of the thickness of our samples, we were able to extract from our k data the dispersion of Sc via KK relations. The sum rules tests indicate an acceptable consistency of the data.

Conclusions

The transmittance of thin films of Sc deposited by evaporation has been measured in situ in the 20-1,000 eV photon energy range in UHV conditions. These transmittance measurements have been used to calculate the extinction coefficient of pure Sc.

The refractive index of Sc in the same energy range has been calculated through the KK dispersion analysis, using the current data along with the data available in the literature. All data used above 7.1 eV come from measurements performed in situ in UHV conditions, except above 1,000 eV, where the Henke semi-empirical approach was used. Below 0.27 eV data from a single uniaxial crystal of Sc was used after performing a refractive index average of the two sets of optical constants, according to a qualitative determination of the crystallites present in a Sc thin film.

The application of two sum-rule tests suggests an acceptable consistency of the KK analysis. We suggest that new in situ characterizations below 7 eV may improve the consistency of the KK analysis.

Acknowledgments

We acknowledge support by the European Community - Research Infrastructure Action under the FP6 "Structuring the European Research Area" Programme (through the Integrated Infrastructure Initiative "Integrating Activity on Synchrotron and Free Electron Laser Science"). This work was also supported by the National Programme for Space Research, Subdirección General de Proyectos de Investigación, Ministerio de Ciencia y Tecnología, project numbers ESP2001-4517-PE and ESP2002-01391. A. M. M. acknowledges the partial support of the Fondo d'Ateneo per la Ricerca (FAR) of Università di Pavia. We acknowledge the technical assistance of José M. Sánchez Orejuela and Víctor Márquez.

References

1. Y. U. Uspenskii, V. E. Levashov, A. V. Vinogradov, A. I. Fedorenko, V. V. Kondratenko, Y. P. Pershin, E. N. Zubarev, V. Y. Fedotov, "High-reflectivity multilayer mirrors for a vacuum-ultraviolet interval of 35-50 nm", *Opt. Lett.* **23**, 771-773 (1998).
2. F. Eriksson, G. A. Johansson, H. M. Hertz, E. M. Gullikson, U. Kreissig, J. Birch, "14.5% near-normal incidence reflectance of Cr/Sc x-ray multilayer mirrors for the water window", *Opt. Lett.* **28**, 2494-2496 (2003).
3. J. H. Weaver and C. G. Olson, "Optical examination of the electronic structure of single-crystal hcp scandium", *Phys. Rev. B* **16**, 731-735 (1977).
4. M. Sigrist, C. Chassaing, J. C. François, F. Antonangeli, N. Zema, M. Piacentini, "Optical properties of scandium thin films", *Phys. Rev. B* **35**, 3760-3764 (1987).
5. B. Brousseau-Lahaye, C. Colliex, J. Frandon, M. Gasgnier, and P. Trebbia, "Determination of the electron excitation spectrum in scandium and yttrium by means of characteristic energy loss measurements", *Phys. Stat. Sol. (b)* **69**, 257-266 (1975).

6. Y. A. Uspenskii, S. V. Antonov, V. Yu, and A. V. Vinogradov, "Optical properties of 3d-transition metals in the spectral interval of interest for discharge pumped XUV lasers", in *Soft X-Ray Lasers and Applications II*, J. J. Rocca, L. B. Da Silva, eds., Proc. SPIE **3156**, 288-294 (1997).
7. Y. A. Uspenskii, J. F. Seely, N. L. Popov, A. V. Vinogradov, Y. P. Pershin, and V. V. Kondratenko, "Efficient method for the determination of extreme-ultraviolet optical constants in reactive materials: application to scandium and titanium", J. Opt. Soc. Am. A **21**, 298-305 (2004).
8. A. L. Aquila, F. Salmassi, E. M. Gullikson, F. Eriksson, J. Birch, "Measurements of the optical constants of scandium in the 50-1300 eV range", in *Optical constants of materials for UV to x-ray wavelengths*, R. Soufli and J. F. Seely, eds., Proc. of SPIE **5538**, 64-71 (2004).
9. J. I. Larruquert, J. A. Aznárez, J. A. Méndez, A. M. Malvezzi, L. Poletto, S. Covini, "Optical properties of Sc films in the far and the extreme ultraviolet", Appl. Opt. **43**, 3271-3278 (2004)
10. R. Verucchi, S. Nannarone, "Triode electron bombardment evaporation source for ultrahigh vacuum thin film deposition", Rev. Sci. Instrum. **71**, 3444-3450 (2000).
11. S. Tolansky, "Multiple-beam interferometry of surfaces and films", Oxford University Press, London, 1948.
12. S. Nannarone, F. Borgatti, A. De Luisa, B. P. Doyle, G. C. Gazzadi, A. Giglia, P. Finetti, N. Mahne, L. Pasquali, M. Pedio, G. Selvaggi, G. Naletto, M. G. Pelizzo, G. Tondello, "The BEAR beamline at ELETTRA", T. Warwick, J. Arthur, H. A. Padmore, J. Stöhr, eds., *AIP Conference Proceedings* **705**, 450-453 (2004).
13. L. Pasquali, A. De Luisa, S. Nannarone, "The UHV Experimental Chamber For Optical Measurements (Reflectivity and Absorption) and Angle Resolved

- Photoemission of the BEAR Beamline at ELETTRA”, T. Warwick, J. Arthur, H.A. Padmore, J. Stöhr, eds., *AIP Conference Proceedings* **705**, 1142-1145 (2004)
14. Absolute XUV silicon photodiode (AXUV series) by International radiation detectors Inc.
15. B.L. Henke, E.M. Gullikson, and J.C. Davis, “X-ray interactions: photoabsorption, scattering, transmission, and reflection at $E=50-30000$ eV, $Z=1-92$ ”, *Atomic Data and Nuclear Data Tables* **54**, 181-342 (1993). These data have been updated after the preparation of this research by including the measurements of Ref. 8.
16. Henke data of Ref. 15 are available at http://www-cxro.lbl.gov/optical_constants/
17. J. H. Weaver, C. Krafska, D. W. Lynch, E. E. Koch, *Physik Daten*, 18-2 (Fachinformationszentrum Energie-Physik-Mathematik GmbH, Karlsruhe, Germany, 1981).
18. M. Gasgnier, Ch. Henry la Blanchetais, P. E. Caro, “Réactivité des métaux des terres rares yttriques et du scandium en couches minces vis-à-vis de l’atmosphère résiduelle du microscope électronique”, *Thin Solid Films*, **31**, 283-295 (1976).
19. B. Sae-Lao, R. Soufli, “Measurements of the refractive index of yttrium in the 50-1300-eV energy region”, *Appl. Opt.* **41**, 7309-7316 (2002).
20. T. G. Mayerhöfer, “New method of modeling infrared spectra of non-cubic single-phase polycrystalline materials with random orientation”, *Appl. Spectrosc.* **56**, 1194-1205 (2002).
21. A tabulated form of the data is available on request at the following email address: larruquert@ifa.cetef.csic.es
22. E. Shiles, T. Sasaki, M. Inokuti, D. Y. Smith, “Self-consistency and sum-rule tests in the Kramers-Kronig analysis of optical data: applications to aluminium”, *Phys. Rev. B* **22**, 1612-1628 (1980).

Table 1. The optical constants at the energies of smallest absorption both below the L and M edges

Energy (eV)	δ	k
27	-0.055	0.024(5)
389.4	-5.0×10^{-4}	$3.0(3) \times 10^{-4}$

Figure captions

Fig. 1: Transmittance of the grid-supported C substrate as a function of the photon energy on a logarithmic scale.

Fig. 2: Transmittance of three scandium films of different thicknesses as a function of the photon energy on a logarithmic scale.

Fig. 3: Logarithm of transmittance as a function of the film thickness at three different energies (symbols) and the fit (solid line).

Fig 4. (Color Online) Log-log plot of the extinction coefficient of Sc obtained with the transmittance measurements, represented along with data in the literature. The spectral range of each set of data is spanned with a straight line.

Fig. 5. (Color Online) The extinction coefficient of Sc at the Sc $L_{2,3}$ edge.

Fig. 6. Log-log plot of the extinction coefficient data set used for the KK analysis

Fig. 7. (Color Online) $\delta=1-n$ in the range of small energies

Fig. 8. (Color Online) Log-log plot of $\delta=1-n$ in the range of large energies

Fig. 9. (Color Online) $\delta=1-n$ at the L edge.

Fig. 10. The effective number of electrons contributing to the extinction coefficient up to each energy

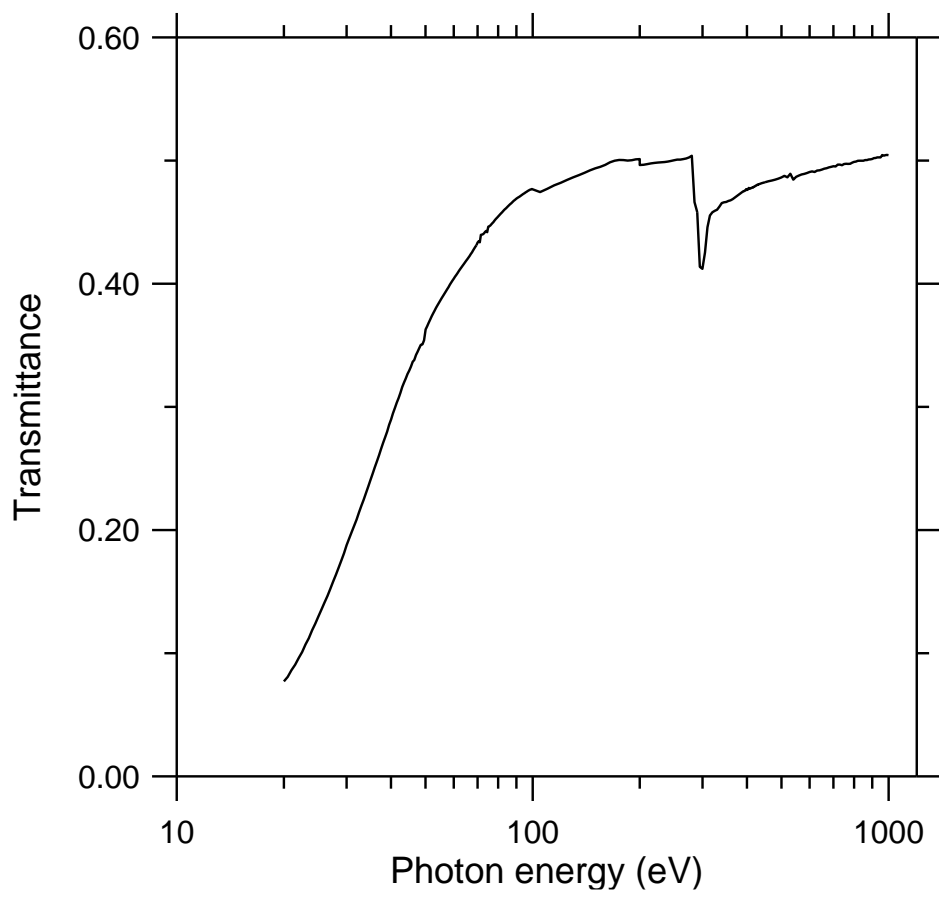


Fig. 1.

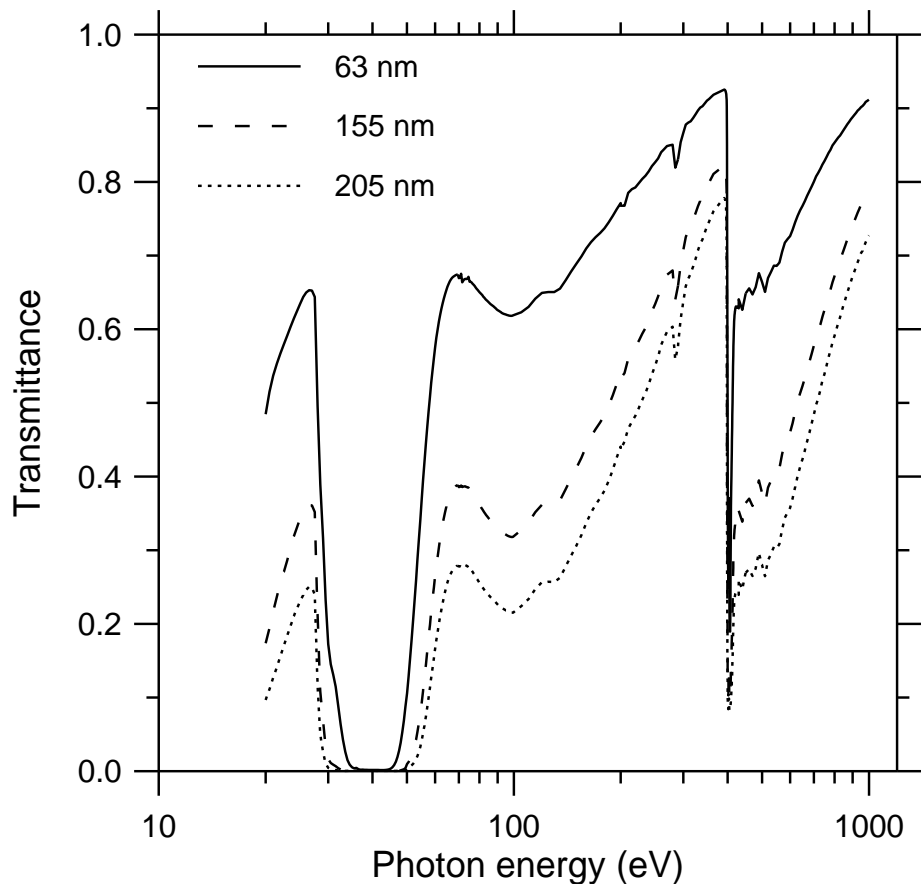


Fig. 2.

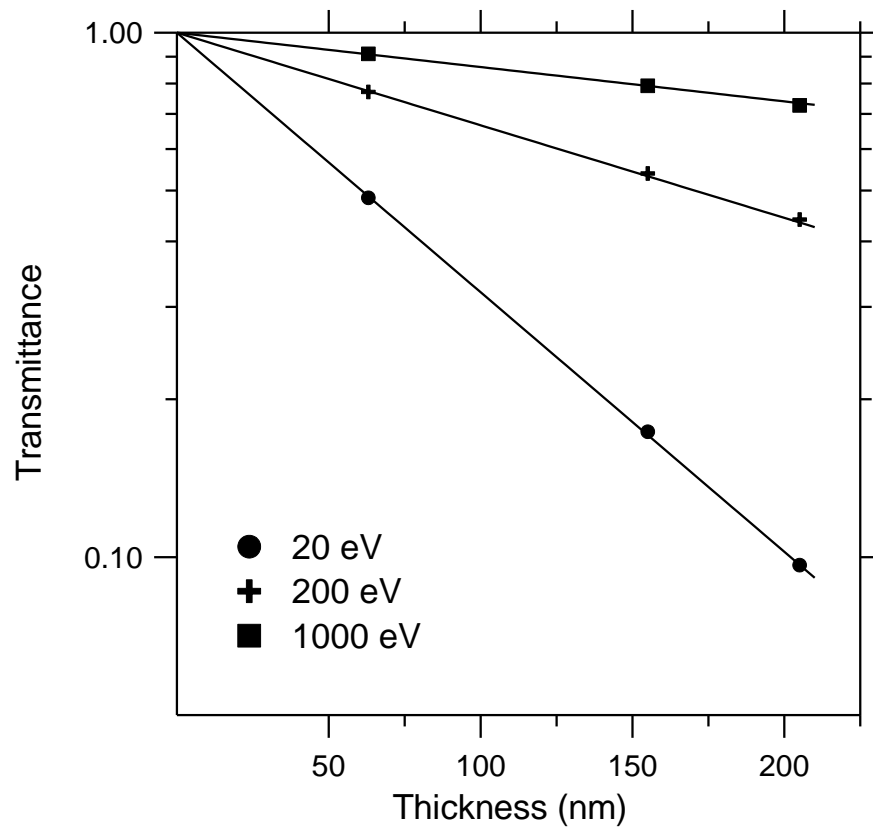


Fig. 3.

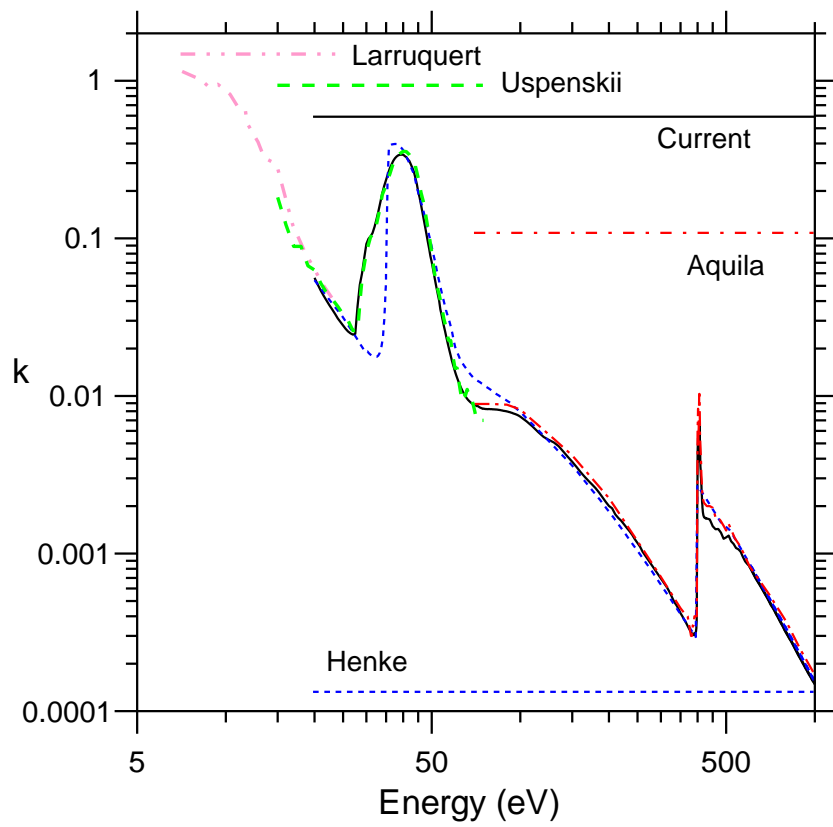


Fig 4.

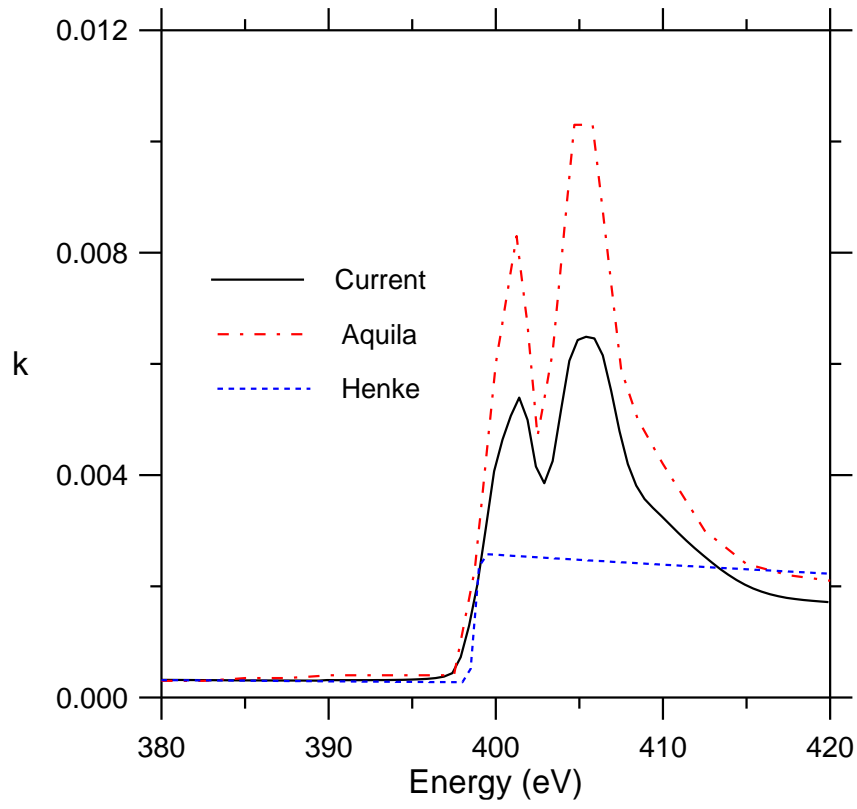


Fig. 5.

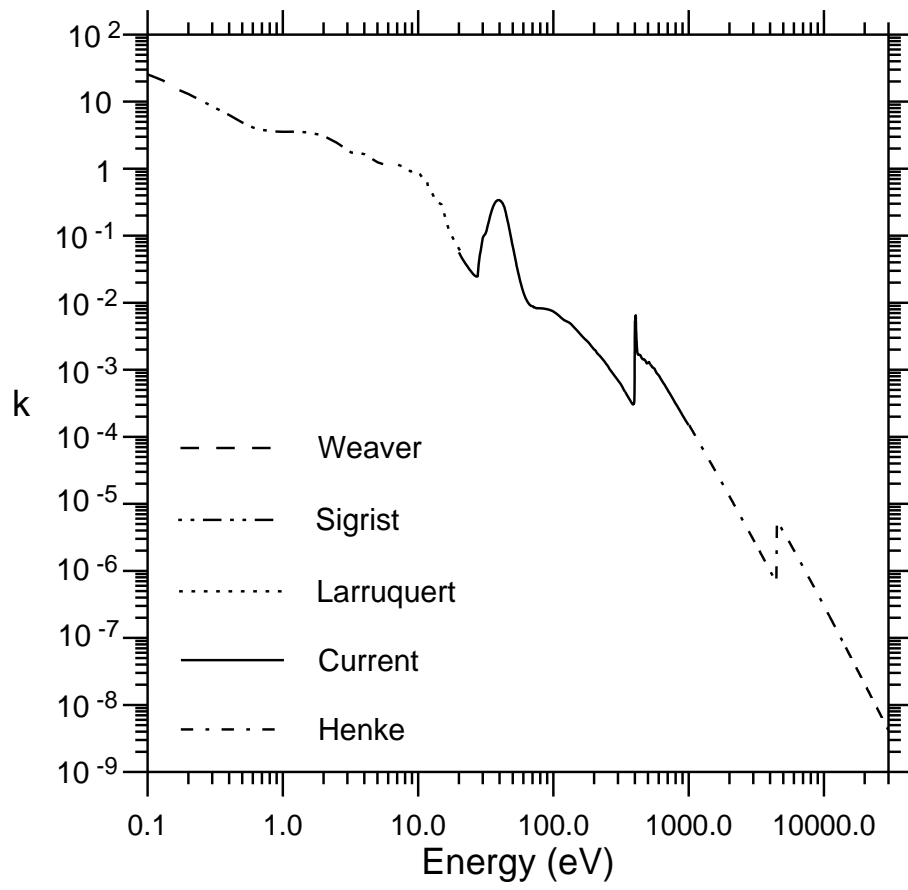


Fig. 6

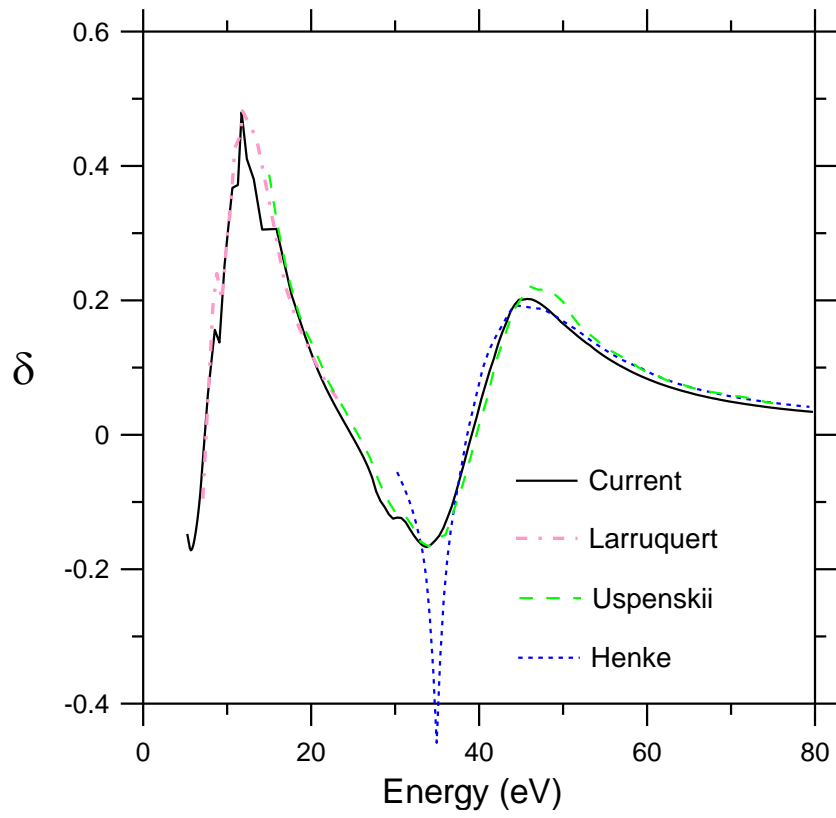


Fig. 7

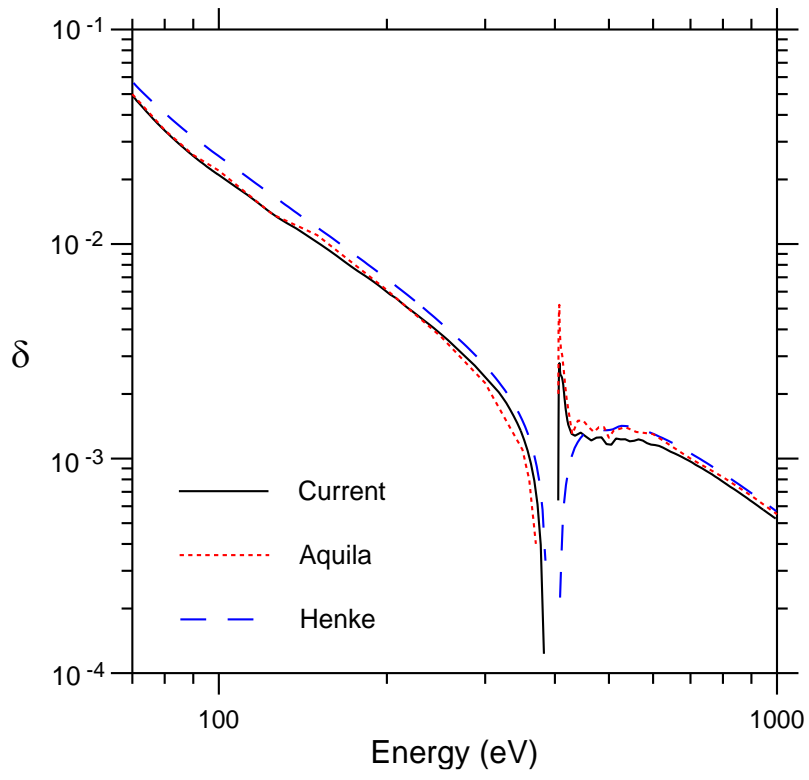


Fig. 8

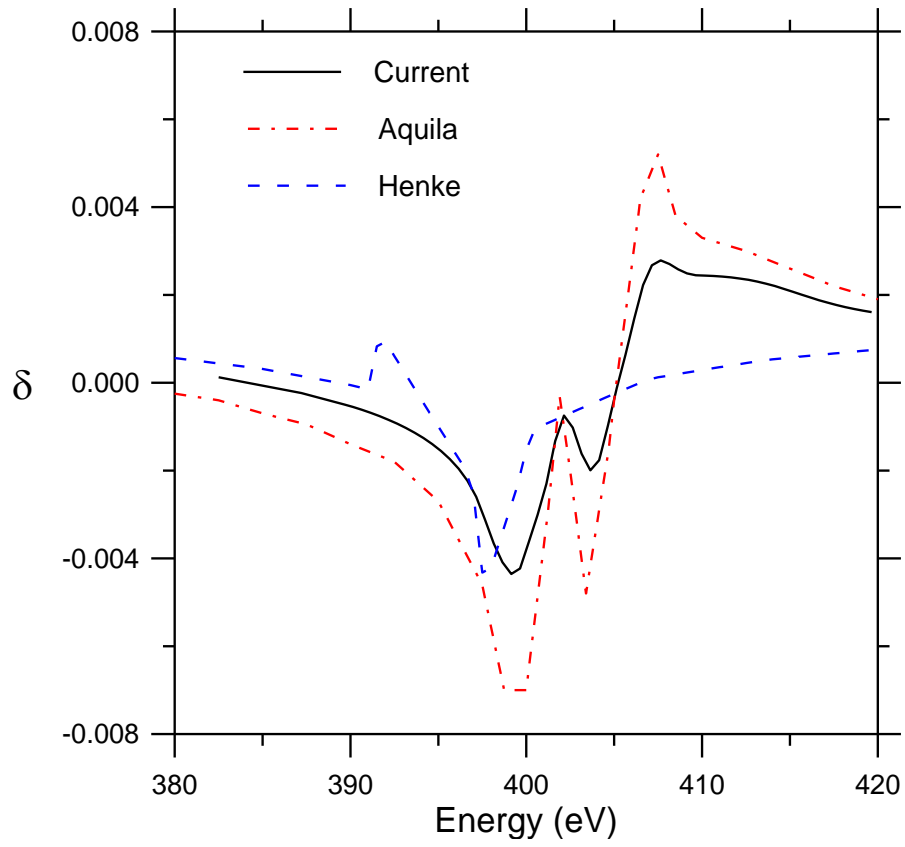


Fig. 9

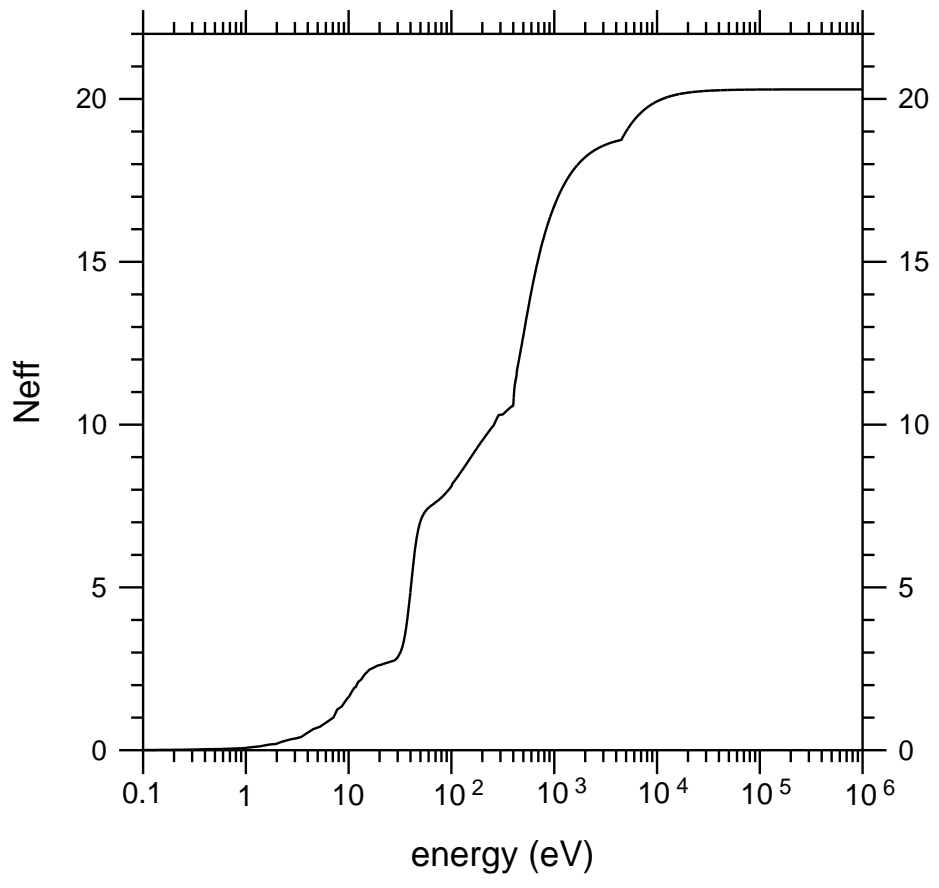


Fig. 10